ASSESSMENT OF THE EFFECTS OF FIRE LOADING ON ACR-1000™ CONTAINMENT STRUCTURE

D. A. Oliveira[1], A. Saudy[2], M. Homam[2], A. Shehata[2], and M. Elgohary[2]
[1]SNC-Lavalin Nuclear Inc., 2275 Upper Middle Road, Oakville, Ontario, Canada L6H 0C3
[2]Atomic Energy of Canada Limited, 2251 Speakman Drive, Mississauga, Ontario, Canada L5K 1B2
E-mail of corresponding author: saudya@aecl.ca

ABSTRACT

The containment structure for the Advanced CANDU Reactor (ACR) 1000 is designed to withstand an impact by a malevolent vehicle (aircraft), as per the requirements of the Canadian Nuclear Safety Commission (CNSC) [1]. In addition to the ability to withstand the dynamic high-rate loads imparted by the aircraft during the collision, the containment structure is expected to experience subsequent thermal loading due to the detonation and deflagration of the fuel within the fuel tank. Based on a review of the literature [2,3] and the requirement by the regulator [1], it is postulated that a portion of the fuel will quickly deflagrate in the form of a fireball with the remainder of the fuel burning in a pool over a longer duration of time. A portion of the heat released from the burning of the aircraft's fuel is absorbed by the containment structure, while the remainder is released to the environment. The effect of this thermal loading on the structural integrity of the containment needs to be assessed. Hence, the objective of this work is to provide an assessment of the structural response of the containment structure due to the postulated loads induced by fire resulting from an impact by an aircraft.

The analysis consists of the implementation of a one-way coupled modeling approach, using the implicit ANSYS [4] finite element software, to simulate the response of the containment structure subjected to thermal loading by the fire. A three-dimensional finite element model of the ACR-1000 containment structure is developed. A thermal finite element analysis is first performed to determine the temperature rise in the concrete due to the thermal loading. The predicted temperature distribution within the containment wall then serves as an input to the subsequent structural finite element analysis that examines the response of the structure to thermal expansion.

The main conclusion from this assessment is that the ACR-1000 containment structure is able to resist the thermal loadings induced by a fire resulting from an impact by an aircraft. The predicted damage to the containment structure is limited to a maximum depth of 42 mm from the outside surface, which is less than the minimum required concrete cover of 60 mm, as specified by the concrete design code [5].

INTRODUCTION

Assessment of Nuclear Civil Structures Exposed to Loading by Fire

There have been a limited number of published studies examining the response of nuclear civil structures exposed to thermal loading by fire resulting from a malevolent act. Furthermore, the studies available within the literature have been limited to assessments based solely on the thermal response to fire without consideration of the stresses and subsequent deformation resulting from the thermal expansion of the various components of the structure. Such an assessment on the containment structure of a CANDU reactor, located at the Gentilly 2 nuclear facility in Quebec, Canada, was performed by Kfoury and Morrison [2]. The assessment was based on a 355 m^2 pool of fuel that yielded 60 minutes of duration for the fire to burn. Kfoury and Morrison concluded that the impact of a fireball on the wall of the containment structure does not induce thermal damage to the building wall, mainly due to the relatively short duration of loading, which was six seconds. They found that the damage induced in the containment structure was mainly due to the burning of the pool of fuel after the fireball. The maximum temperature in the concrete was 883 K (610 ºC) and the depth of damage from the outer wall was 40 mm. A damage threshold of 773 K (500 ºC) was utilized to identify portions of the concrete wall that had lost some load carrying capacity, which was not specified. Within the literature, there exists a variation in the relative strength of concrete as a function of temperature. For the threshold temperature of 773 K (500 ºC) used in the Gentilly 2 analysis, the strength of concrete reported in the literature decreases by roughly 10% to 50% depending on the mixture [6,7,8,9].

An evaluation of the response of a pressurized heated water nuclear containment exposed to fire resulting from an impact by an aircraft was performed by Kiran *et al*. [3]. They performed a transient thermal finite element analysis and the main conclusion was that the outer concrete cover would be severely damaged, while the remainder

of the wall would experience little temperature rise. They also found that the fireball has a negligible effect on the wall of the outer containment building.

Thermal Load Due to Fire

The thermal loading on the containment structure was determined based on the guidelines provided by the International Atomic Energy Agency (IAEA) [10] and US-NRC Nuclear Regulatory Guideline (NUREG 1805) [11], and is expressed in terms of heat flux. A total of six different load cases were determined based on a total mass of jet fuel of 225,000 kg and 0%, 25% and 50% of the fuel forming into a fireball prior to burning of the fire pool and are shown in Table 1. The first three cases consider one-quarter of the containment structure exposed to the heat flux, while the last three cases consider one-half of the containment exposed, as shown in Fig. 1. Note that the subscript associated with the various points of reference denotes the region of exposure to heat flux. The pool of fire is assumed to form on the roof of the reactor auxiliary building (RAB), which limits the loading to predominantly the dome region of the containment structure. Note that the flux is linearly interpolated between the various points of reference. For brevity, the most severe results from the assessment, which corresponds to the examination of load case 1, will be focused upon in this paper.

Table 1: Fire load cases considered in the assessment.

Load Case	Region of Exposure of containment structure	FIRE BALL								FIRE POOL							
		Duration [seconds]	Flux [kW/m^2]							Duration [minutes]	Flux [kW/m^2]						
			A	A'	B	B'	C	C'	D		A	A'	B	B'	C	C'	D
1	One-Quarter	0	0	0	0	0	0	0	0	44	15	20	25	25	15	20	15
2		14	70	70	70	70	70	70	90	33	15	20	25	25	15	20	15
3		16	70	75	75	75	70	75	90	22	15	20	25	25	15	20	15
4	One-Half	0	0	0	0	0	0	0	0	22	20	30	25	25	20	30	25
5		14	70	70	70	70	70	70	90	16	20	30	25	25	20	30	25
6		16	70	75	75	75	70	75	90	11	20	30	25	25	20	30	25

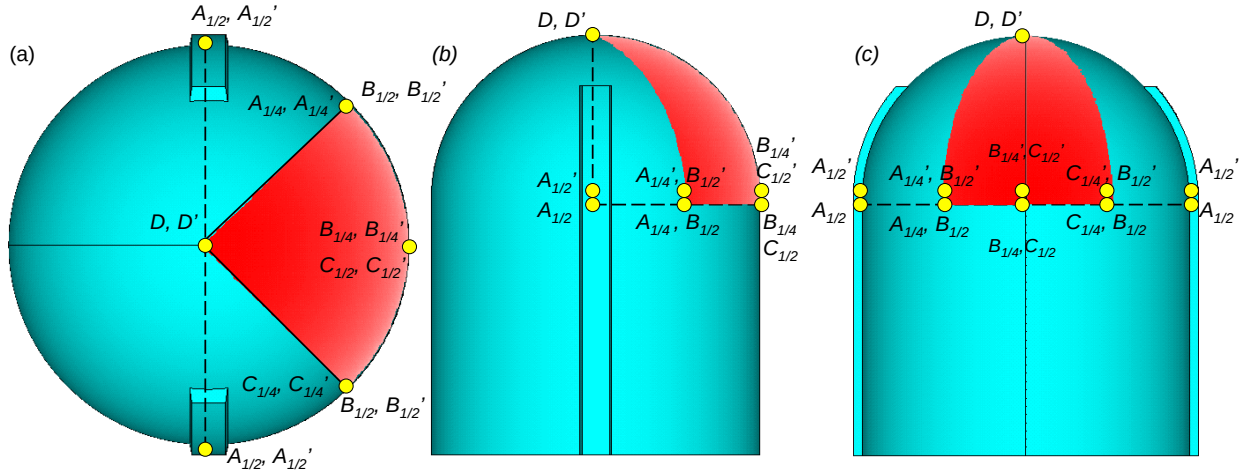

Fig. 1: Region of containment structure exposed to heat flux. The case of one-quarter exposure is highlighted

NUMERICAL MODEL

Overview

The ANSYS version 11 finite element software [4] was adopted as the tool to conduct the analysis. The strategy to analyzing the response of the containment structure subjected to loading by fire is summarized in Figure 2. A steady-state thermal analysis is first performed based on the temperature boundary conditions corresponding to the summer season that is considered and the temperature distribution throughout the containment structure is determined. The initial temperature distribution within the containment structure and the fire load, represented by the heat flux, serve as input parameters for the transient thermal analysis that is performed. The nodal temperatures

at the point of the most severe gradient of temperature serve as an input into the steady state structural analysis, which also considers the steel liner, reinforcement, prestressing of the tendons and loads due to gravity. Finally, the stresses, strains and deflection of the containment structure is determined and examined in terms of structural integrity.

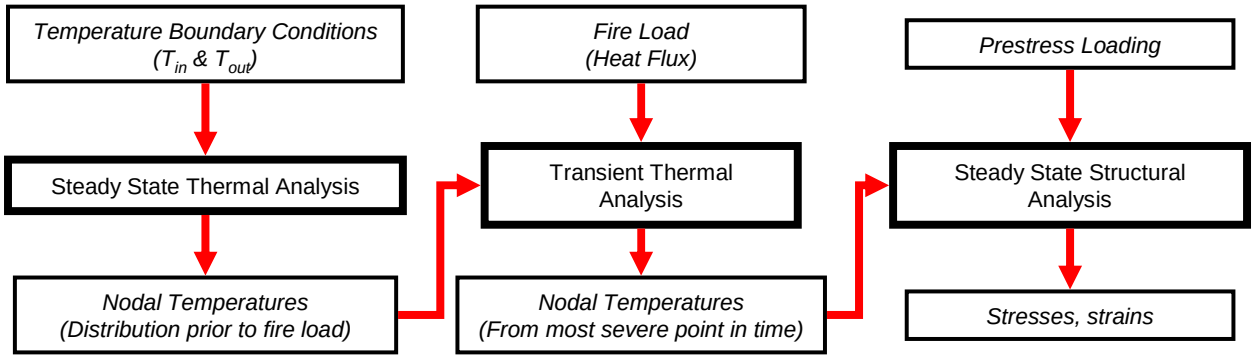

Figure 2: Flow chart of the simulation approach for the three-dimensional model

In order to assess the structural response of the containment structure to thermal loading, two simplified approaches are utilized. The first approach, considers the response of the concrete to loading arising from thermal expansion. The assessment of the containment structure's ability to resist these loads represents a conservative approach since in actuality the concrete experiences localized cracking that prevents load transfer generated from thermal expansion to the surrounding concrete. The second approach, investigates the structural response of the containment structure to resist the prestress and self-weight loadings when the damaged concrete sections have entirely lost their load-carrying capability. In order to mimic this scenario, the elements attached to nodes with a temperature greater than a threshold value are deleted from the simulation prior to conducting the structural analysis. The threshold of temperature implemented is 773 K (500 ºC. The implementation of these two approaches results in an overall conservative analysis of the containment structure's response to thermal loading; however, it has the advantage of significantly promoting convergence of the non-linear implicit solver.

Material Properties

The material parameters used to characterize the thermal conduction characteristics of concrete include: thermal conductivity, specific heat and density. The non-linear thermal properties of concrete were adopted from the Eurocode EN 1992-1-2 [12] and are

$$k^{upper}(T) = 2.0 - 0.2451(T/100) + 0.0107(T/100)^2 \quad \text{[W/mK]} \tag{1}$$

$$k^{lower}(T) = 1.36 - 0.136(T/100) + 0.0057(T/100)^2 \quad \text{[W/mK]} \tag{2}$$

$$c(T) = \begin{cases} 900 & [J/kgK] \quad T \le 100^oC \\ 900 + (T-100) & [J/kgK] \quad 100^oC < T \le 200^oC \\ 1000 + (T-200)/2 & [J/kgK] \quad 200^oC < T \le 400^oC \\ 1100 & [J/kgK] \quad 400^oC < T \le 1200^oC \end{cases} \tag{3}$$

$$\rho(T) = \begin{cases} \rho(20^oC) & T \le 115^oC \\ \rho(20^oC)(1 - 0.02(T-115)/85) & 115^oC < T \le 200^oC \\ \rho(20^oC)(0.98 - 0.03(T-200)/200) & 200^oC < T \le 400^oC \\ \rho(20^oC)(0.95 - 0.07(T-400)/800) & 400^oC < T \le 1200^oC \end{cases} \tag{4}$$

The thermal conductivity is linearly interpolated between the upper and lower bounds defined by Equation 1 and 2 to have a value of 1.7 W/mK at T=0 K. The rebars, tendons and steel liner are not considered in the thermal analysis since any significant temperature rise within the containment wall is small relative to the thickness of the wall [2, 3].

The material parameters used to characterize the structural response of concrete include: modulus of elasticity (32 GPa); density (2,400 kg/m^3); Poisson's ratio (0.15) and the coefficient of thermal expansion (0.00001

m/m/K). For simplicity, a bilinear elasto-plastic material model is utilized in the three-dimensional models. The unconfined compressive strength of the concrete (*fc'*) that was considered is 45.7 MPa and was determined based on the ACI code [13], and the tangent modulus was set to zero (i.e. perfectly plastic). Note that the bilinear isotropic material model within ANSYS does not consider the different yield stress in compression and tension; hence, the response of the concrete in tension is treated as linearly elastic until *fc'*. The idealization of the constitutive response of concrete was found to be advantageous in promoting convergence of the solver, while providing a more realistic treatment than simply linearly elastic in nature. Typical material properties for steel were assigned to the linear elastic material models used to represent the rebars, tendons and liner.

Finite Element Representation

The finite element discretization of the containment structure is shown in Fig. 3a. A one-half symmetry representation of the structure is examined that does not consider the RAB. Refinement of the mesh in the through thickness direction within the area of loading was necessary to better capture the temperature gradient in the wall resulting from the fire. For the thermal analysis, the 20-noded high-order solid brick element formulation (SOLID90 in ANSYS) is utilized to represent the outer layers of elements representing the concrete, while the 8-noded lower-order solid brick element formulation (SOLID70) comprised the remainder of the concrete. For the structural analysis, the 20-noded (SOLID95) and 8-noded (SOLID45) solid brick element formulations were utilized for the corresponding high- and low-order elements, respectively.

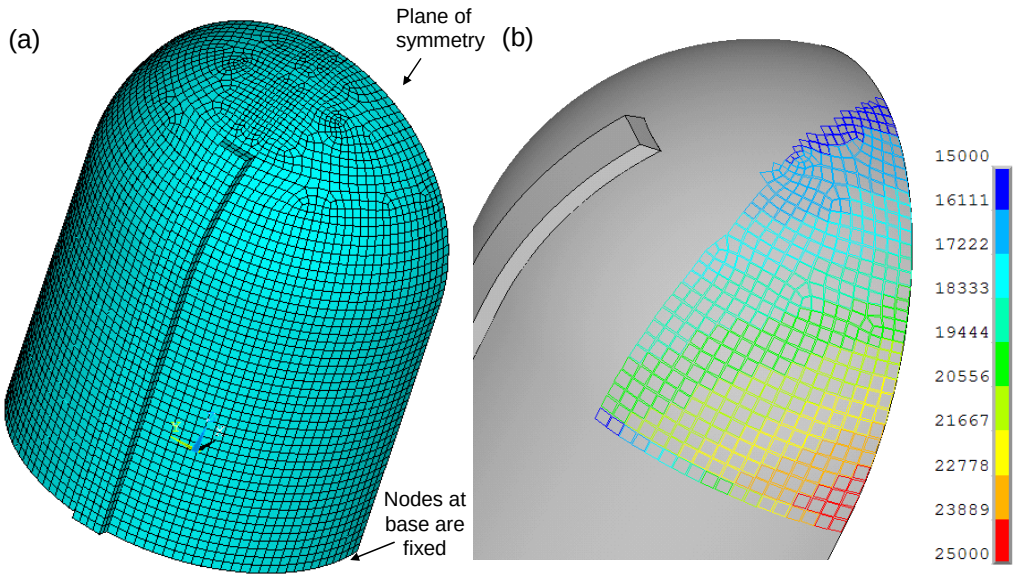

Fig. 3: (a) Finite element representation of the containment structure; and, (b) contours of applied heat flux (W/m^2)

Boundary Conditions and Loading

The maximum temperature within the inside and outside of the containment structure prior to exposure to fire is considered to be 322 K (49 ºC) and 309 K (36 ºC), respectively. The contours of the applied heat flux on the outer surface of the containments structure is shown in Fig. 3b. The nodes at the base of containment are fully constrained in all three directions, and appropriate boundary constraints are applied to the rebars and tendons to capture the coupled nature of the interaction with the concrete elements. The loading of the hoop- and vertical-tendons that provide prestress to the concrete is generated through the application of a temperature decrease in the tendon that induces the desired compressive stress in the concrete.

RESULTS

Effect of Thermal Expansion

The predicted contours of temperature within the containment structure due to the heat flux loading are shown in Fig. 4a. The distribution of temperature induced in the dome of the containment structure is consistent with the distribution of the applied heat flux, which was shown in Fig. 3b. The lowest temperature in the containment structure is 309 K (36 ºC), which corresponds to the lowest temperature prior to exposure to heat flux.

The maximum temperature of the concrete is 1157 K (884 ºC). The contours of von Mises stress predicted to occur in the containment structure at the point of most severe thermal loading is shown in Fig. 4b. The maximum stress developed within the containment structure occurs within the first outer layer of elements in the loaded region of the dome.

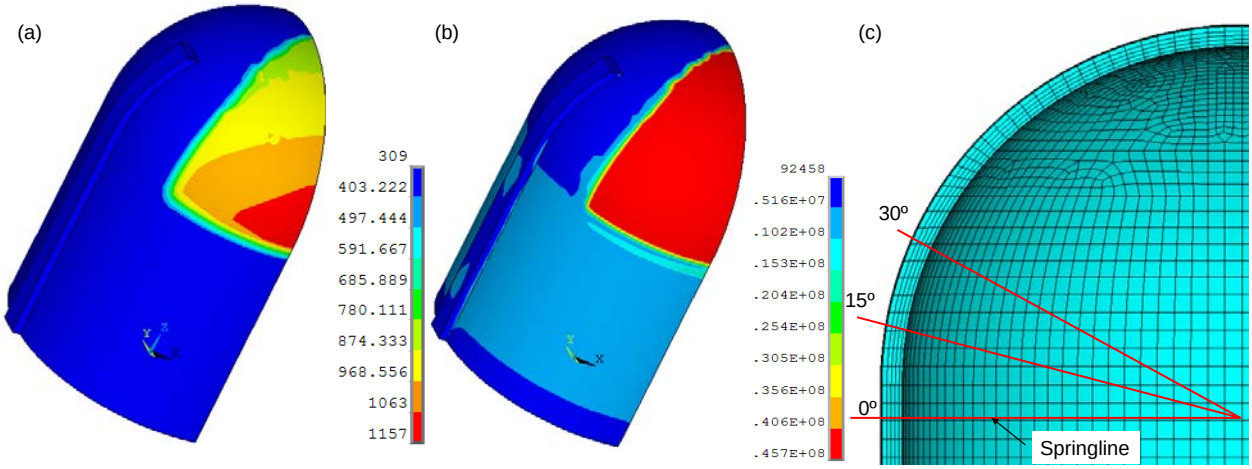

Fig. 4: (a) Contours of temperature (K); (b) contours of von Mises stress (Pa); and, (c) location of dome sections

In order to assess the effect of the fire on the stresses within the dome, the meridian (circumferential in vertical plane) and hoop (circumferential in horizontal plane) stresses are examined in the region of highest load at sections of the wall corresponding to 0-, 15- and 30-degrees to the horizontal plane defined by the interface between the dome and wall (i.e. springline), as shown in Fig. 4c. Note that the stresses in elements at the plane of symmetry are examined. The predicted meridian and hoop stress in the 0-, 15- and 30-degree sections of the wall when loaded and not loaded with heat flux from the fire are shown in Fig. 5. The loading of the containment structure with heat flux resulting from a fire causes a reduction in the compressive stresses within the sections of the wall up to 108 mm from the outside surface. The reduction in compressive stress is a consequence of the thermal expansion of the concrete, which loads the surrounding concrete in tension. The maximum tensile stress observed is 3.8 MPa, which is below the tensile strength of concrete estimated as 4.2 MPa according to the ACI code [14]. The compressive stresses in the concrete that extend beyond the ultimate compressive strength (*fc'*) occur within roughly 42 mm from the wall and are expected to result in localized damage of the concrete.

Structural Integrity of Damaged Containment Structure

The predicted contours of von Mises stress within the containment structure due to the temperature distribution shown in Fig. 4a and neglecting the region of concrete exposed to a temperature greater than the threshold of 773 K (500 ºC) is shown in Fig. 6. The distribution of stress is consistent with the case where the entire concrete is considered (Fig. 4b), with the exception that the high stresses are now limited to the top region of the dome that experiences a maximum temperature less than the threshold.

The stress at the 0-, 15-, and 30-degree locations of the dome in the meridional and hoop directions corresponding to the loading condition that does not consider the concrete sections above the threshold temperature is shown in Fig. 6. Also shown is the corresponding stress considering the entire concrete within the dome. The absence of the layer of concrete above the threshold temperature alleviates the tensile stresses developed due to thermal expansion and results in an overall lower stress within the dome. The resultant stress within the wall lies within the elastic bounds of concrete stress given by the tensile and unconfined compressive strength.

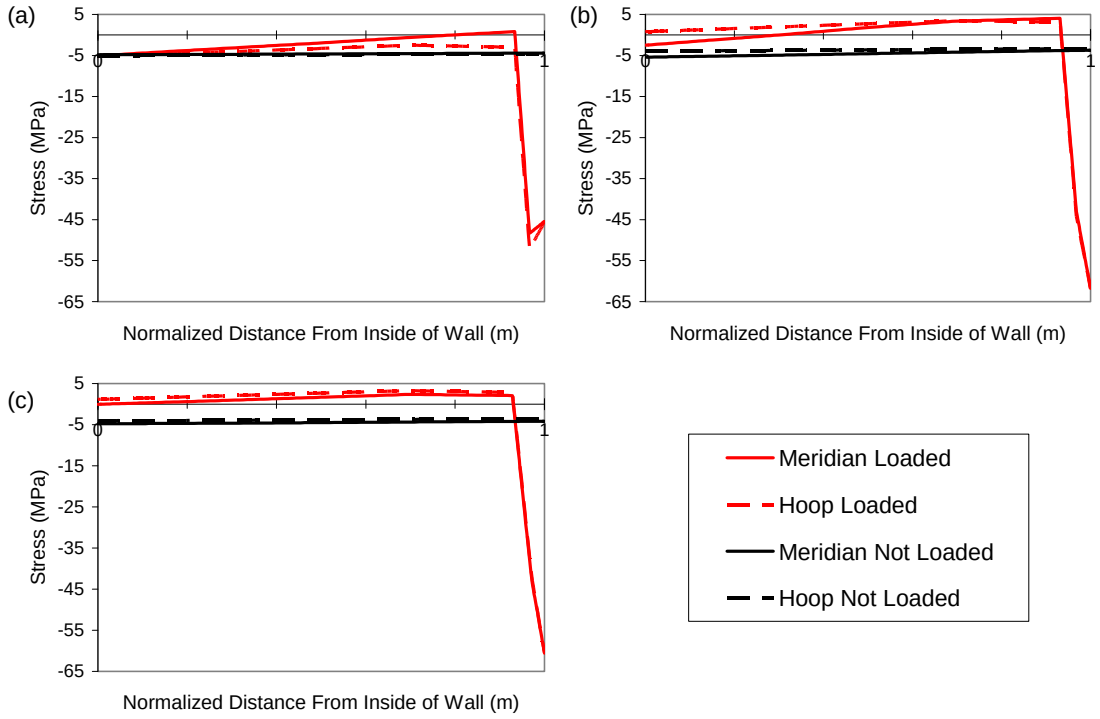

Fig. 5: Meridianal and hoop stress through the dome wall at the (a) 0; (b) 15; and (c) 30-degree locations

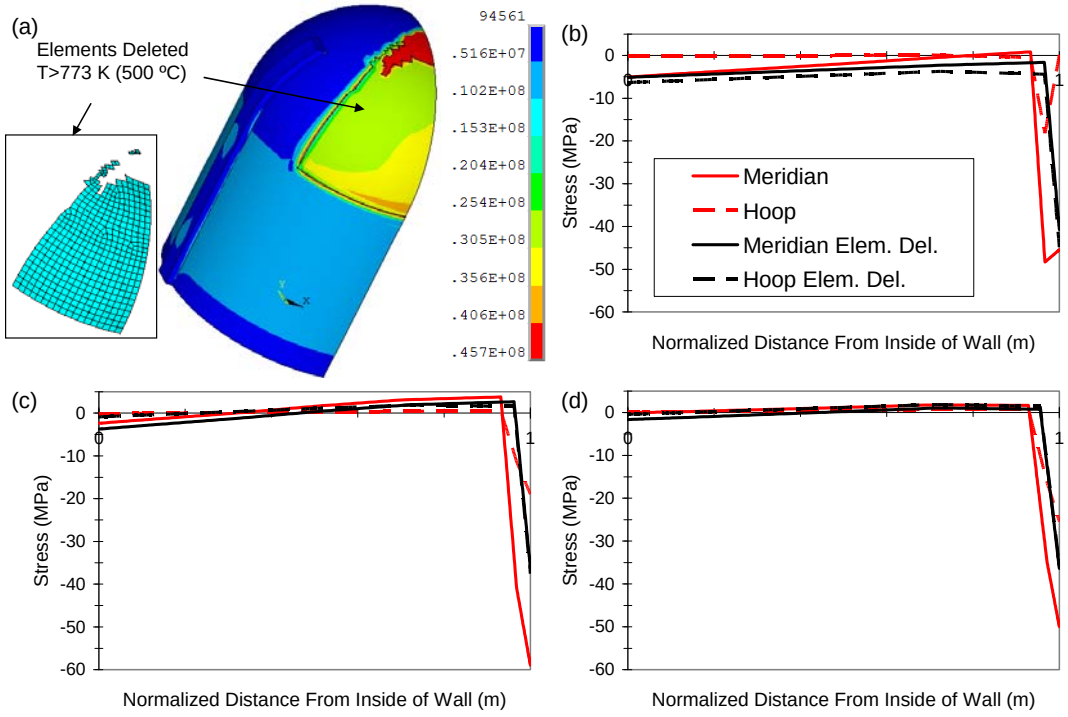

Fig. 6: (a) Contours of von Mises stress developed within containment structure without regions of concrete above threshold temperature (Pa). Meridianal and hoop stress through the dome wall at the (b) 0; (c) 15; and (d) 30-degree locations.

DISCUSSION AND CONCLUSIONS

The effect of a fire resulting from the impact of a malevolent vehicle onto the containment structure of the ACR-1000 has been assessed based on several fire loading scenarios, for which that most severe case was presented in this paper. A loosely-coupled modeling approach was implemented that consisted of a transient thermal analysis to determine the temperature distribution within the structure resulting from the heat flux generated by the fire. The most severe distribution of temperature within the concrete was identified and served as an input into the steady state structural analysis of the containment structure that also considered the effects of prestressing of the tendons, as well as loads generated by gravity.

Although none of the load cases comprised of loading by a fireball were not explicitly presented within this paper, the maximum temperature rise within the concrete exposed to the fireball was found to be 190-degrees. The rise in temperature of the concrete due to the fireball is relatively modest considering that the fireball consumed 50% of the fuel within less than one-third of a minute. The most severe case of loading of the containment structure occurs when the entire fuel is burned within a pool over a longer duration and a fireball does not form. The resultant maximum stress within the section of the containment structure was closest to the tensile strength of concrete, which indicates an increased likelihood of localized cracking, when the pool of fire was limited to one-quadrant of the containment structure.

A simplified approach consisting of an elastic-perfectly plastic constitutive response that did not consider cracking was used to represent concrete in the structural analysis. The simplification of the concrete's constitutive response from a sophisticated and highly non-linear material model to a bilinear model allowed for significant gains in computational efficiency to be achieved. The consequence of this simplified treatment of the concrete behaviour results in a conservative estimate of the stress in the containment structure since the concrete thermally expands without cracking. In actuality, the localized cracking of concrete reduces the load transfer capability to surrounding regions; hence, the predictions of stress are conservatively overestimated and represent an upper bound. The lower bound for the stresses within the containment structure was obtained by neglecting the load transfer capability of the region of concrete that experiences a temperature rise above the threshold value of 773 K (500 ºC. The actual meridional and hoop stress developed within the containment structure is expected to lie between these two bounds, which predict stresses less than the tensile strength of concrete. Localized cracking of the concrete subjected to fire loading is estimated to occur within 42 mm of the outside surface for load case 1 (i.e. the most severe). The minimum required cover for concrete exposed to fire required by the CSA Standard CAN/CSA-A23.1 [14] is 60 mm, which limits the estimated cracking depth to the concrete cover and not beyond the outer layer of reinforcing bars. The maximum predicted temperature at 60 mm from the surface exposed to the fire is roughly 550 K (277 ºC), and would not significantly reduce the yield stress of any potential steel rebar, as per the Eurocode EN1992-1-2 [12].

The main conclusion from this assessment is that a concrete cover of 60 mm, as required by the CSA standard [14], will provide adequate protection to the containment structure to resist the loadings induced by fire with damage mainly limited to the concrete cover.

REFERENCES

[1] RD-337 Regulatory Document. Design of New Nuclear Power Plants. Canadian Nuclear Safety Commission. September 2008.

[2] I. Kfoury, L. Morrison. Gentilly 2 Nuclear Containment Structure Modelling of Fire Loading. One-Day Workshop, February 11, 2004, Extreme Loadings, Aging and Durability of Concrete Structures. Organized and sponsored by Hydro-Quebec, McGill University and Laboratoire de Beton.

[3] A.R. Kiran, K.A. Rao, M.K. Agrawal, R.K. Singh, A.K. Ghosh and H.S. Kushwaha. Evaluation of Containment Response for Fire Load due to Aircraft Fuel Spillage. 20th International COncference on Structural Mechanics in Reactor Technology (SMiRT 20), Espoo, Finland, August 9-14, 2009, SMiRT 20-Division 4, Paper 1805.

[4] ANSYS Inc. www.ansys.com

[5] CSA-A23.1/A23.2, "Concrete Materials and Methods of Concrete Construction/Methods of Test and Standard Practices for Concrete"

[6] Mindness, S., Young, J.F. and Darwin, D., Concrete, Second Edition, Prentice Hall, Upper Saddle River, New Jersey, 664p.

[7] Arioz, O., Effects of elevated temperature on the properties of concrete. Fire Safety Journal, Vol. 42, N8, November 2007, pp. 516-522.
[8] Neville, A.M. Properties of concrete, Fourth Edition. Pearson Education Limited.
[9] Mehta, P.K., Monteiro, P.J.M., Concrete microstructure, properties and materials, Third Edition, McGraw-Hill.
[10] International Atomic Energy Agency (IAEA), Protection of Nuclear Power Plants Against Extreme External Events Including Those of Malevolent Origin, IAEA-TECDOC-XXXX, Draft Revision 10, April 21, 2008.
[11] NUREG 1805, Fire Dynamics Tools (FDTs), Quantitative Fire Hazard Analysis Methods for the U.S. Nuclear Regulatory Commission Fire Protection Inspection Program, Final Report, December 2004.
[12] BS EN 1992-1-2, Eurocode 2. Design of concrete structures. General rules. Structural fire design.
[13] ACI 318-05 Building Code Requirements for Structural Concrete and Commentary, Committee 318.
[14] CSA-A23.1/A23.2, "Concrete Materials and Methods of Concrete Construction/Methods of Test and Standard Practices for Concrete"